

Gaussian processes with linear operator inequality constraints

Christian Agrell

Department of Mathematics

University of Oslo

P.O. Box 1053 Blindern, Oslo N-0316, Norway

CHRISAGR@MATH.UIO.NO

Group Technology and Research

DNV GL

P.O. Box 300, 1322 Høvik, Norway

Pre-print

Abstract

This paper presents an approach for constrained Gaussian Process (GP) regression where we assume that a set of linear transformations of the process are bounded. It is motivated by machine learning applications for high-consequence engineering systems, where this kind of information is often made available from phenomenological knowledge, and the resulting constraints may be essential to achieve the level of confidence needed. We consider a GP f over functions on $\mathcal{X} \subset \mathbb{R}^n$ taking values in \mathbb{R} , where the process $\mathcal{L}f$ is still Gaussian when \mathcal{L} is a linear operator. Our goal is to model f under the constraint that realizations of $\mathcal{L}f$ are confined to a convex set of functions. In particular we require that $a \leq \mathcal{L}f \leq b$ given two functions a and b where $a < b$ pointwise. This formulation provides a consistent way of encoding multiple linear constraints, such as shape-constraints based on e.g. boundedness, monotonicity or convexity as a relevant example. We adopt the approach of using a sufficiently dense set of virtual observation locations where the constraint is required to hold, and derive the exact posterior for a conjugate likelihood. The results needed for stable numerical implementation are derived, together with an efficient sampling scheme for estimating the posterior process which is exact in the limit. A few numerical examples focusing on noiseless observations are given. This is relevant for computer code emulation and is also more computationally demanding than the alternative scenario with i.i.d. Gaussian noise.

Keywords: Gaussian processes, uncertainty quantification, linear constraints

1. Introduction

Gaussian Processes (GPs) are a flexible tool for Bayesian nonparametric function estimation, and widely used for applications that require inference on functions such as regression and classification. A useful property of GPs is that they automatically produce estimates on prediction uncertainty, and it is often possible to encode prior knowledge in a principled manner in the modelling of prior covariance. Some early well-known applications of GPs are within spatial statistics, e.g. meteorology (Thompson, 1956), and in geostatistics (Matheron, 1973) where it is known as *kriging*. More recently GPs have become a popular

choice within probabilistic machine learning (Rasmussen and Williams, 2005; Ghahramani, 2015). Since the GPs can act as interpolators when observations are noiseless, GPs have also become the main approach for uncertainty quantification and analysis involving computer experiments (Sacks et al., 1989; Kennedy and O’Hagan, 2001)

Often, the modeler performing function estimation has prior knowledge, or at least hypotheses, on some properties of the function to be estimated. This is typically related to the function shape with respect to some of the input parameters, such as boundedness, monotonicity or convexity. Various methods have been proposed for imposing these types of constraints on GPs (see Section 4 for a short review). For engineering and physics based applications constraints based on integral operators and partial differential equations are also relevant (Jidling et al., 2017; Särkkä, 2011). What the above constraints have in common is that they are linear operators, and so any combination of such constraints can be written as a single linear operator. For instance, the constraints $a_1(\mathbf{x}) \leq f(\mathbf{x}) \leq b_1(\mathbf{x})$, $\partial f/\partial x_i \leq 0$ and $\partial^2 f/\partial x_j^2 \geq 0$ for some function (or distribution over functions) $f : X \rightarrow Y$, can be written as $a(\mathbf{x}) \leq \mathcal{L}f(\mathbf{x}) \leq b(\mathbf{x})$ for $a(\mathbf{x}) = [a_1(\mathbf{x}), -\infty, 0]^T$, $b(\mathbf{x}) = [b_1(\mathbf{x}), 0, \infty]^T$ and $\mathcal{L} : Y^X \rightarrow (Y^X)^3$ being the linear operator $\mathcal{L}f = [f, \partial f/\partial x_i, \partial^2 f/\partial x_j^2]^T$.

The motivation for including these constraints on GPs is usually to improve predictions and to obtain a reduced and more realistic estimate on the uncertainty, the latter having significant impact for risk-based applications. For many real-world systems information related to constraints in this form is often available from phenomenological knowledge. For engineering systems this is typically knowledge related to some underlying physical phenomenon. Being able to make use of these constraint in probabilistic modelling is particularly relevant for high-consequence applications, where obtaining realistic uncertainty estimates in subsets of the domain where data is scarce is a challenge. Furthermore, information on whether these types of constraints are likely to hold given a set of observations is also useful for explainability and model falsification. For a broader discussion see (Agrell et al., 2018) and (Eldevik et al., 2018).

In this paper we present a model for estimating a function $f : \mathbb{R}^N \rightarrow \mathbb{R}$ by a constrained GP (CGP) $f|D, a(\mathbf{x}) \leq \mathcal{L}f(\mathbf{x}) \leq b(\mathbf{x})$, where D is a set of observations of (\mathbf{x}_j, y_j) , possibly including additive white noise, and $f \sim \mathcal{GP}(\mu(\mathbf{x}), K(\mathbf{x}, \mathbf{x}'))$ is a GP with mean $\mu(\mathbf{x})$ and covariance function $K(\mathbf{x}, \mathbf{x}')$ that are chosen such that existence of $\mathcal{L}f$ is ensured. Due to the linearity of \mathcal{L} , both $\mathcal{L}f|D$ and $f|D, \mathcal{L}f$ remain Gaussian, and our approach is based on modelling $f|D, \mathcal{L}f$ under the constraint $a(\mathbf{x}) \leq \mathcal{L}f(\mathbf{x}) \leq b(\mathbf{x})$. To model the constraint that $a(\mathbf{x}) \leq \mathcal{L}f(\mathbf{x}) \leq b(\mathbf{x})$ for all inputs \mathbf{x} , we take the approach of using a finite set of input locations where the constraint is required to hold. That is, we require that $a(\mathbf{x}_v) \leq \mathcal{L}f(\mathbf{x}_v) \leq b(\mathbf{x}_v)$ for a finite set of inputs $\{\mathbf{x}_v\}$ called the set of *virtual observation locations*. With this approach the CGP is not guaranteed to satisfy the constraint on the entire domain, but a finite set of points $\{\mathbf{x}_v\}$ can be found so that the constraint holds globally with sufficiently high probability.

The model presented in this paper is inspired by the research on shape constrained GPs (Wang and Berger, 2016; Golchi et al., 2015; Riihimäki and Vehtari, 2010; Lenk and Choi, 2017; Da Veiga and Marrel, 2012, 2015; Maatouk and Bay, 2017; López-Lopera et al., 2018; Abrahamsen and Benth, 2001; Lin and Dunson, 2014), and the need for a simple framework for imposing multiple such constraints. In the case where $\mathcal{L} = \partial/\partial x_i$ our approach is most similar to that in (Wang and Berger, 2016), where the authors make use of a similar

sampling scheme for noiseless GP regression applied to computer code emulation. With the exception of (Maatouk and Bay, 2017; López-Lopera et al., 2018), most of the approaches to constrained GPs (including ours) rely on the constraint to be satisfied at a specified set of virtual locations. The use of virtual constraint observations may seem *ad hoc* at first, as the set of virtual observation locations has to be dense enough to ensure that the constraint holds globally with sufficiently high probability. Inversion of the covariance matrix of the joint GP may therefore be of concern, both because this scales with the number of observations cubed and because there is typically high serial correlation if there are many virtual observations close together. The general solution is then to restrict the virtual observation set to regions where the probability of occurrence of the constraint is low (Riihimäki and Vehtari, 2010; Wang and Berger, 2016). According to Wang and Berger (2016), when they followed this approach in their experiments they found that only a modest number of virtual observations were typically needed and that these points were usually rather disperse and the resulting serial correlation was not severe. There is also one benefit with the virtual observation approach, which is that implementation of constraints that only hold on subsets of the domain is straightforward.

For practical use of the model presented in this paper we also pay special attention to numerical implementation. The computations involving only real observations or only virtual observations are separated, which is convenient when only changes to the constraints are made such as in algorithms for finding a sparse set of virtual observation locations or for testing/validation of constraints. We also provide the algorithms based on Cholesky factorization for stable numerical implementation, and an efficient sampling scheme for estimating the posterior process and for finding an optimal set of virtual observation locations. These algorithms are based on derivation of the exact posterior of the constrained Gaussian process using a general linear operator, and constitutes the main contribution of this paper.

The paper is structured as follows: In Section 2 we state the results needed on GP regression and GPs under linear transformations. Our main results are given in Section 3 where we introduce the constrained GP (CGP) and present the model for GP regression under linear inequality constraints. In particular, given some training data we derive the posterior distribution of the CGP evaluated at a finite set of inputs, which is a compound Gaussian with a truncated Gaussian mean (Section 3.1). Section 3.2 presents an algorithm for sampling from the posterior, and parameter estimation is addressed in Section 3.3. Section 3.4 and Section 3.5 are dedicated to optimization of the set of virtual observation locations needed to ensure that the constraint holds with sufficiently high probability. Finally, numerical examples considering monotonicity and boundedness constraints are presented in Section 4, and some concluding remarks are given in Section 5.

2. Gaussian processes and linear operators

We are interested in GP regression on functions $f : \mathbb{R}^{n_x} \rightarrow \mathbb{R}$ under the additional inequality constraint $a(\mathbf{x}) \leq \mathcal{L}f(\mathbf{x}) \leq b(\mathbf{x})$ for some specified functions $a(\mathbf{x})$ and $b(\mathbf{x})$, and the class of linear operators $\{\mathcal{L}|\mathcal{L}f : \mathbb{R}^{n_x} \rightarrow \mathbb{R}^{n_c}\}$. Here n_x and n_c are positive integers, and the subscripts are just used to indicate the relevant underlying space over \mathbb{R} . We will make use of the properties of GPs under linear transformations given below.

2.1 Gaussian process regression

We consider a Gaussian process $f \sim \mathcal{GP}(\mu(\mathbf{x}), K(\mathbf{x}, \mathbf{x}'))$ given as a prior over functions $f : \mathbb{R}^{n_x} \rightarrow \mathbb{R}$, which is specified by its mean and covariance function

$$\begin{aligned} \mu(\mathbf{x}) &= \mathbb{E}[f(\mathbf{x})] : \mathbb{R}^{n_x} \rightarrow \mathbb{R}, \\ K(\mathbf{x}, \mathbf{x}') &= \mathbb{E}[(f(\mathbf{x}) - \mu(\mathbf{x}))(f(\mathbf{x}') - \mu(\mathbf{x}'))] : \mathbb{R}^{n_x \times n_x} \rightarrow \mathbb{R}. \end{aligned} \tag{1}$$

Let \mathbf{x} denote a vector in \mathbb{R}^{n_x} and X the $n_x \times N$ matrix of N such input vectors. The distribution over the vector \mathbf{f} of N latent values corresponding to X is then multivariate Gaussian with

$$\mathbf{f}|X \sim \mathcal{N}(\mu(X), K(X, X)),$$

where $K(X, X')$ denotes the Gram matrix $K(X, X')_{i,j} = K(\mathbf{x}_i, \mathbf{x}'_j)$ for two matrices of input vectors X and X' . Given a set of observations $Y = [y_1, \dots, y_N]^T$, and under the assumption that the relationship between the latent function values and observed output is Gaussian, $Y|\mathbf{f} \sim \mathcal{N}(\mathbf{0}, \sigma^2 I_N)$, the predictive distribution for new observations X^* is still Gaussian with mean and covariance

$$\begin{aligned} \mathbb{E}[\mathbf{f}^*|X^*, X, Y] &= \mu(X^*) + K(X^*, X)[K(X, X) + \sigma^2 I_N]^{-1}(Y - \mu(X)), \\ \text{cov}(\mathbf{f}^*|X^*, X, Y) &= K(X^*, X^*) - K(X^*, X)[K(X, X) + \sigma^2 I_N]^{-1}K(X, X^*). \end{aligned} \tag{2}$$

Here $\mathbf{f}^*|X^*$ is the predictive distribution of $f(X^*)$ and $\mathbf{f}^*|X^*, X, Y$ is the predictive posterior given the data X, Y . For further details see e.g. Rasmussen and Williams (2005).

2.2 Linear operations on Gaussian processes

Let \mathcal{L} be a linear operator on realizations of $f \sim \mathcal{GP}(\mu(\mathbf{x}), K(\mathbf{x}, \mathbf{x}'))$. As GPs are closed under linear operators (Rasmussen and Williams, 2005; Papoulis and Pillai, 2002), $\mathcal{L}f$ is still a GP¹. We will assume that the operator produces functions with range in \mathbb{R}^{n_c} , but where the input domain \mathbb{R}^{n_x} is unchanged. That is, the operator produces functions from \mathbb{R}^{n_x} to \mathbb{R}^{n_c} . This type of operators on GPs has also been considered by Särkkä (2011) with applications to stochastic partial differential equations. The mean and covariance of $\mathcal{L}f$ are given by applying \mathcal{L} to the mean and covariance of the argument

$$\begin{aligned} \mathbb{E}[\mathcal{L}f(\mathbf{x})] &= \mathcal{L}\mu(\mathbf{x}) : \mathbb{R}^{n_x} \rightarrow \mathbb{R}^{n_c}, \\ \text{cov}(\mathcal{L}f(\mathbf{x}), \mathcal{L}f(\mathbf{x}')) &= \mathcal{L}_1 \mathcal{L}_2^T K(\mathbf{x}, \mathbf{x}') : \mathbb{R}^{n_x \times n_x} \rightarrow \mathbb{R}^{n_c \times n_c}, \end{aligned}$$

1. We assume here that $\mathcal{L}f$ exists. For instance, if \mathcal{L} involves differentiation then the process f must be differentiable. See e.g. (Adler, 1981) for details on proving existence.

and the cross-covariance is given as

$$\begin{aligned}\text{cov}(\mathcal{L}f(\mathbf{x}), f(\mathbf{x}')) &= \mathcal{L}_1 K(\mathbf{x}, \mathbf{x}') : \mathbb{R}^{n_x \times n_x} \rightarrow \mathbb{R}^{n_c}, \\ \text{cov}(f(\mathbf{x}), \mathcal{L}f(\mathbf{x}')) &= \mathcal{L}_2^T K(\mathbf{x}, \mathbf{x}') : \mathbb{R}^{n_x \times n_x} \rightarrow \mathbb{R}^{n_c}.\end{aligned}$$

The notation \mathcal{L}_i for $i = 1, 2$ here means that the operator acts on $K(\mathbf{x}, \mathbf{x}')$ as a function of the i -th parameter keeping the other one fixed, i.e. $\mathcal{L}K(\mathbf{x}, \cdot)$ for $i = 1$ and $\mathcal{L}K(\cdot, \mathbf{x}')$ for $i = 2$. The transpose operator is defined as $\mathcal{L}_i^T K(\mathbf{x}, \mathbf{x}') = (\mathcal{L}_i K(\mathbf{x}, \mathbf{x}'))^T$. In the following sections we make use of the predictive distribution (2) where observations correspond to the transformed GP under \mathcal{L} .

3. Gaussian processes with linear inequality constraints

Following Section 2.1 and Section 2.2, we let $f \sim \mathcal{GP}(\mu(\mathbf{x}), K(\mathbf{x}, \mathbf{x}'))$ be a GP over real valued functions on \mathbb{R}^{n_x} , and \mathcal{L} a linear operator producing functions from \mathbb{R}^{n_x} to \mathbb{R}^{n_c} . The matrix X and the vector Y will represent N noise perturbed observations: $y_i = f(\mathbf{x}_i) + \varepsilon_i$ with ε_i i.i.d. $\mathcal{N}(0, \sigma^2)$ for $i = 1, \dots, N$.

We would like to model the posterior GP conditioned on the observations X, Y , and on the event that $a(\mathbf{x}) \leq \mathcal{L}f(\mathbf{x}) \leq b(\mathbf{x})$ for two functions $a(\mathbf{x}), b(\mathbf{x}) : \mathbb{R}^{n_x} \rightarrow (\mathbb{R} \cup \{-\infty, \infty\})^{n_c}$ where $a_i(\mathbf{x}) < b_i(\mathbf{x})$ for all $\mathbf{x} \in \mathbb{R}^{n_x}$ and $i = 1, \dots, n_c$. To achieve this approximately we start by assuming that the constraint $a(\mathbf{x}) \leq \mathcal{L}f(\mathbf{x}) \leq b(\mathbf{x})$ only holds at a finite set of inputs $\mathbf{x}_1^v, \dots, \mathbf{x}_{N_v}^v$ which we refer to as *virtual observation locations*. Later we will consider how to specify the set of virtual observation locations such that the initial constraint defined for all \mathbf{x} holds with sufficiently high probability. Furthermore, we will also assume that *virtual observations* of the transformed process, $\mathcal{L}f(\mathbf{x}_i^v)$, comes with additive white noise with variance σ_v^2 . We can write this as $a(X^v) \leq \mathcal{L}f(X^v) + \varepsilon^v \leq b(X^v)$ where $X^v = [\mathbf{x}_1^v, \dots, \mathbf{x}_{N_v}^v]^T$ is the matrix containing the virtual observation locations and ε^v is a multivariate Gaussian with diagonal covariance of elements σ_v^2 .

We will make use of the following notation: Let $\tilde{C}(X^v) \in \mathbb{R}^{N_v \times n_c}$ be the matrix with rows $(\tilde{C}(X^v))_i = \mathcal{L}f(\mathbf{x}_i^v) + \varepsilon_i^v$ for i.i.d. $\varepsilon_i^v \sim \mathcal{N}(\mathbf{0}, \sigma_v^2 I_{n_c})$, and let $C(X^v)$ denote the event $C(X^v) := \bigcap_{i=1}^{N_v} \{a(\mathbf{x}_i^v) \leq (\tilde{C}(X^v))_i \leq b(\mathbf{x}_i^v)\}$. $C(X^v)$ thus represents the event that the constraint $a(\mathbf{x}) \leq \mathcal{L}f(\mathbf{x}) + \varepsilon^v \leq b(\mathbf{x})$ is satisfied for all points in X^v , and it is defined through the latent variable $\tilde{C}(X^v)$.

In summary, the process we will consider is stated as

$$f|X, Y, X^v, C(X^v) := f|f(X) + \varepsilon = Y, a(X^v) \leq \mathcal{L}f(X^v) + \varepsilon^v \leq b(X^v),$$

where f is a Gaussian process, X, Y is the training data and X^v are the locations where the transformed process $\mathcal{L}f$ is bounded. The additive noise ε and ε^v are multivariate Gaussian with diagonal covariance matrices of elements σ^2 and σ_v^2 respectively.

Here we assume that observations of all parts of $\mathcal{L}f$ comes with i.i.d. white noise with variance σ_v^2 . The reason for this is mainly for numerical stability where we in computations will choose a tiny variance to approximate noiseless observations. Similarly, σ^2 may be chosen as a fixed small number for interpolation in the standard GP regression setting. In the following derivations, the results for exact noiseless observations can be obtained by setting

the relevant variance to zero. We also assume that any sub-operator of \mathcal{L} is constrained at the same set of virtual locations X^v . This is mainly for notational convenience, and this assumption is easily relaxed (see Section 3.5).

3.1 Posterior predictive distribution

Our goal is to obtain the posterior predictive distribution $\mathbf{f}^*|X^*, X, Y, X^v, C(X^v)$. That is: the distribution of $\mathbf{f}^* = f(X^*)$ for some new inputs X^* , conditioned on the observed data $Y = f(X) + \varepsilon$ and the constraint $a(X^v) \leq \mathcal{L}f(X^v) + \varepsilon^v \leq b(X^v)$.

To simplify the notation we write $\mathbf{f}^*|Y, C$, excluding the dependency on inputs X, X^* and X^v (as well as any hyperparameter of the mean and covariance function). The posterior predictive distribution is given by marginalizing over the latent variable \tilde{C} :

$$p(\mathbf{f}^*, C|Y) = p(\mathbf{f}^*|C, Y)p(C|Y),$$

$$p(\mathbf{f}^*|C, Y) = \int_{a(X^v)}^{b(X^v)} p(\mathbf{f}^*|\tilde{C}, Y)p(\tilde{C}|Y)d\tilde{C},$$

$$p(C|Y) = \int_{a(X^v)}^{b(X^v)} p(\tilde{C}|Y)d\tilde{C},$$

where the limits correspond to the hyper-rectangle in $\mathbb{R}^{N_v \times n_c}$ given by the functions $a(\cdot)$ and $b(\cdot)$ evaluated at each $\mathbf{x}^v \in X^v$. The predictive distribution and the probability $p(C|Y)$ are given in Lemma 1. $p(C|Y)$ is of interest, as it is the probability that the constraint holds at X^v given the data Y .

In the remainder of the paper we will use the shortened notation $\mu^* = \mu(X^*)$, $\mu = \mu(X)$, $\mu^v = \mu(X^v)$ and $K_{X, X'} = K(X, X')$. For vectors with elements in \mathbb{R}^{n_c} , such as $\mathcal{L}\mu^v$, we interpret this elementwise; $\mathcal{L}\mu^v(X^v) = [\mathcal{L}\mu(\mathbf{x}_1^v)_1, \dots, \mathcal{L}\mu(\mathbf{x}_1^v)_{n_c}, \dots, \mathcal{L}\mu(\mathbf{x}_{N_v}^v)_1, \dots, \mathcal{L}\mu(\mathbf{x}_{N_v}^v)_{n_c}]^T$

Lemma 1 *The predictive distribution $\mathbf{f}^*|Y, C$ is a compound Gaussian with truncated Gaussian mean:*

$$\mathbf{f}^*|Y, C \sim \mathcal{N}(\mu^* + A(\mathbf{C} - \mathcal{L}\mu^v) + B(Y - \mu), \Sigma), \quad (3)$$

$$\mathbf{C} = \tilde{C}|Y, C \sim \mathcal{TN}(\mathcal{L}\mu^v + A_1(Y - \mu), B_1, a(X^v), b(X^v)), \quad (4)$$

where $\mathcal{TN}(\cdot, \cdot, a, b)$ is the Gaussian $\mathcal{N}(\cdot, \cdot)$ conditioned on the hyper-rectangle $[a_1, b_1] \times \dots \times [a_k, b_k]$, and

$$\begin{aligned}
A_1 &= (\mathcal{L}_1 K_{X^v, X})(K_{X, X} + \sigma^2 I_N)^{-1}, \\
A_2 &= K_{X^*, X}(K_{X, X} + \sigma^2 I_N)^{-1}, \\
B_1 &= \mathcal{L}_1 \mathcal{L}_2^T K_{X^v, X^v} + \sigma_v^2 I_{N_v n_c} - A_1 \mathcal{L}_2^T K_{X, X^v}, \\
B_2 &= K_{X^*, X^*} - A_2 K_{X, X^*}, \\
B_3 &= \mathcal{L}_2^T K_{X^*, X^v} - A_2 \mathcal{L}_2^T K_{X, X^v}, \\
A &= B_3 B_1^{-1}, \\
B &= A_2 - A A_1, \\
\Sigma &= B_2 - A B_3^T.
\end{aligned}$$

Moreover, the constraint probability $p(C|Y)$ is the probability that the unconstrained version of \mathbf{C} falls within the constraint region, i.e.

$$p(C|Y) = p(a(X^v) \leq \mathcal{N}(\mathcal{L}\mu^v + A_1(Y - \mu), B_1) \leq b(X^v)), \quad (5)$$

and the unconstrained predictive distribution is

$$\mathbf{f}^*|Y \sim \mathcal{N}(\mu + A_2(Y - \mu), B_2).$$

The derivation in Lemma 1 is based on conditioning the multivariate Gaussian $(\mathbf{f}^*, Y, \tilde{C})$, and the proof is given in Appendix A. For practical implementation the matrix inversions involved in Lemma 1 may be prone to numerical instability. A numerically stable alternative is given in Lemma 2.

In the following lemma $\text{Chol}(K)$ is the lower triangular Cholesky factor of a matrix K . We also let $R = (P \setminus Q)$ denote the solution to the linear system $PR = Q$ for matrices P and Q , which may be efficiently computed when P is triangular using forward or backward substitution.

Lemma 2 Let $L = \text{Chol}(K_{X, X} + \sigma^2 I_N)$, $v_1 = L \setminus \mathcal{L}_2^T K_{X, X^v}$ and $v_2 = L \setminus K_{X, X^*}$.

Then the matrices in Lemma 1 can be computed as

$$\begin{aligned}
A_1 &= (L^T \setminus v_1)^T, \\
A_2 &= (L^T \setminus v_2)^T, \\
B_1 &= \mathcal{L}_1 \mathcal{L}_2^T K_{X^v, X^v} + \sigma_v^2 I_{N_v n_c} - v_1^T v_1, \\
B_2 &= K_{X^*, X^*} - v_2^T v_2, \\
B_3 &= \mathcal{L}_2^T K_{X^*, X^v} - v_2^T v_1.
\end{aligned}$$

Moreover, B_1 is symmetric and positive definite. By letting $L_1 = \text{Chol}(B_1)$ and $v_3 = L_1 \setminus B_3^T$ we also have

$$\begin{aligned}
A &= (L_1^T \setminus v_3)^T, \\
B &= A_2 - AA_1, \\
\Sigma &= B_2 - v_3^T v_3.
\end{aligned}$$

The numerical complexity of the procedures in Lemma 2 is $n^3/6$ for Cholesky factorization of $n \times n$ matrices and $mn^2/2$ for solving triangular systems where the unknown matrix is $n \times m$. In the derivation of Lemma 1 and Lemma 2 the order of operations was chosen such that the first cholesky factor $L = \text{Chol}(K_{X,X} + \sigma^2 I_N)$ only depends on X . This is convenient in the case where the posterior $\mathbf{f}^*|Y, C$ is calculated multiple times for different constraints C or virtual observations X^v , but where the data X, Y remain unchanged. For such computations using $X^{v,1}, \dots, X^{v,m}$ where $X^{v,j}$ contains $N_{v,j}$ observations the numerical complexity is $\mathcal{O}(N^3) + \mathcal{O}(n_c^3 \sum_j N_{v,j}^3)$.

3.2 Sampling from the posterior distribution

In order to sample from the posterior we can first sample from the constraint distribution (4), and then use these samples in the mean of (3) to create the final samples of $\mathbf{f}^*|Y, C$.

To generate m samples of the posterior at k new input locations, $[\mathbf{x}_1^*, \dots, \mathbf{x}_k^*]^T = X^*$, we use the following procedure

Algorithm 3 *Sampling from the posterior distribution*

1. Find a matrix Q s.t. $Q^T Q = \Sigma \in \mathbb{R}^{k \times k}$, e.g. by Cholesky or a spectral decomposition.
2. Generate \tilde{C}_m , a $N_v n_c \times m$ matrix where each column is a sample of $\tilde{C}|Y, C$ from the distribution in (4).
3. Generate U_m , a $k \times m$ matrix with m samples from the standard normal $\mathcal{N}(\mathbf{0}, I_k)$.
4. The $k \times m$ matrix where each column is a sample from $\mathbf{f}^*|Y, C$ is then obtained by

$$[\mu^* + B(Y - \mu)] \oplus_{\text{col}} [A(-\mathcal{L}\mu^v \oplus_{\text{col}} \tilde{C}_m) + QU_m],$$

where \oplus_{col} means that the $k \times 1$ vector on the left hand side is added to each column of the $k \times m$ matrix on the right hand side.

This procedure is based on the well-known method for sampling from multivariate Gaussian distributions, where we have used the property that in the distribution of $\mathbf{f}^*|Y, C$, only the mean depends on samples from the constraint distribution.

The challenging part of this procedure is the second step where samples have to be drawn from a truncated multivariate Gaussian. The simplest approach is by rejection sampling, i.e. generating samples from the normal distribution and rejection those that fall outside the bounds. In order to generate m samples with rejection sampling, the expected number of samples needed is $m/p(C|Y)$, where the acceptance rate is the constraint probability $p(C|Y)$ given in (5). If the acceptance rate is low then rejection sampling becomes inefficient, and alternative approaches such as Gibbs sampling (Kotecha and Djuric, 1999) is typically

used. In our numerical experiments (presented in Section 4) we made use of a new method based on simulation via minimax tilting developed by Botev (2017). Note also that when sampling from the posterior for a new set of input locations X^* , when the data X, Y and virtual observation locations X^v are unchanged, the samples generated in step 2 may be reused.

3.3 Parameter estimation

To estimate the parameters of the CGP we make use of the marginal maximum likelihood approach (MLE). We define the marginal likelihood function of the CGP as

$$L(\theta) = p(Y, C|\theta) = p(Y|\theta)p(C|Y, \theta), \quad (6)$$

i.e. as the probability of the data Y and constraint C combined, given the set of parameters represented by θ . We assume that both the mean and covariance function of the GP prior (1) $\mu(\mathbf{x}|\theta)$ and $K(\mathbf{x}, \mathbf{x}'|\theta)$ may depend on θ .

The log-likelihood, $l(\theta) = \ln p(Y|\theta) + \ln p(C|Y, \theta)$, is thus given as the sum of the unconstrained log-likelihood, $\ln p(Y|\theta)$, which is optimized in unconstrained MLE, and $\ln p(C|Y, \theta)$ which is the probability that the constraint holds at X^v given in (5). When the constraint probability $p(C|Y, \theta)$ is computed using Lemma 2, the unconstrained part of the likelihood is also given by

$$\ln p(Y|\theta) = -v^T v - \text{tr}(L) - \frac{n}{2} \ln 2\pi \quad (7)$$

for $v = L \setminus (Y - \mu)$ (see e.g. Rasmussen and Williams, 2005). It is often reasonable to assume the maximum marginal likelihood estimate of θ , $\hat{\theta}_{MLE} = \arg \max L(\theta)$, should be close to the unconstrained estimate given by maximizing (7), in which case using the unconstrained estimate as an initial guess in numerical optimization should be an efficient strategy. For numerical optimization of (6) it might also be beneficial to make use of the gradient of the marginal log-likelihood. This involves differentiation of $\ln p(C|Y, \theta)$ which could be done by making use of the first two moments of a truncated multivariate Gaussian (Lee and Scott, 2012), and the derivatives of the covariance function w.r.t. θ .

In (Bachoc et al., 2018) the authors study the asymptotic distribution of the MLE for shape-constrained GPs, and show that for large sample sizes the effect of including the constraint in the MLE is negligible. But for small or moderate sample sizes the constrained MLE is generally more accurate so taking the constraint into account is beneficial. In the numerical experiments presented in this paper we make use of the unconstrained MLE as an initial guess, and to find the set of virtual observation locations needed to impose the constraint with high probability (see Section 3.4). When the set of virtual locations has been determined the MLE can be updated where the constraint probability is included.

3.4 Finding the virtual observations

For the constraint to be satisfied locally at any input location in some bounded set $\Omega \subset \mathbb{R}^{n_x}$ with sufficiently high probability, the set of virtual observation locations X^v has to be sufficiently dense. We will specify a target probability $p_{\text{target}} \in [0, 1)$ and find a set X^v such that when the constraint is satisfied at all virtual locations in X^v , the probability that the

constraint is satisfied for any \mathbf{x} in Ω is at least p_{target} . The number of virtual observations needed depends on the smoothness properties of the kernel, and for a given kernel it is of interest to find a set X^v that is effective in terms of numerical computation. As we need to sample from a truncated Gaussian involving cross-covariances between all elements in X^v , this means that we would like the set X^v to be small as well as avoiding points in X^v close together that could lead to high serial correlation.

Seeking an optimal set of virtual observations has also been discussed in (Wang and Berger, 2016; Golchi et al., 2015; Riihimki and Vehtari, 2010; Da Veiga and Marrel, 2012, 2015) and the intuitive idea is to iteratively place virtual observations where the probability that the constraint holds is low. The general approach presented in this section is most similar to that in (Wang and Berger, 2016). In Section 3.5 we extend this to derive a more efficient algorithm for multiple constraints.

In order to estimate the probability that the constraint holds at some new location $\mathbf{x}^* \in \Omega$ we first derive the posterior distribution of the constraint process.

Lemma 4 *The predictive distribution of the constraint $\mathcal{L}f(\mathbf{x}^*)$ for some new input $\mathbf{x}^* \in \mathbb{R}^{n_x}$, condition on the data Y is given by*

$$\mathcal{L}f(\mathbf{x}^*)|Y \sim \mathcal{N}(\mathcal{L}\mu^* + \tilde{A}_2(Y - \mu), \tilde{B}_2), \quad (8)$$

and when $\mathcal{L}f(\mathbf{x}^*)$ is conditioned on both the data and virtual constraint observations, X, Y and $X^v, C(X^v)$, the posterior becomes

$$\mathcal{L}f(\mathbf{x}^*)|Y, C \sim \mathcal{N}(\mathcal{L}\mu^* + \tilde{A}(C - \mathcal{L}\mu^v) + \tilde{B}(Y - \mu), \tilde{\Sigma}). \quad (9)$$

Here L, v_1, A_1, B_1 and L_1 are defined as in Lemma 2, C is the distribution in (4) and

$$\begin{aligned} \tilde{v}_2 &= L \setminus \mathcal{L}_2^T K_{X, \mathbf{x}^*}, \\ \tilde{A}_2 &= (L^T \setminus \tilde{v}_2)^T, \\ \tilde{B}_2 &= \mathcal{L}_1 \mathcal{L}_2^T K_{\mathbf{x}^*, \mathbf{x}^*} - \tilde{v}_2^T \tilde{v}_2, \\ \tilde{B}_3 &= \mathcal{L}_1 \mathcal{L}_2^T K_{\mathbf{x}^*, X^v} - \tilde{v}_2^T v_1, \\ \tilde{v}_3 &= L_1 \setminus \tilde{B}_3^T, \\ \tilde{A} &= (L_1^T \setminus \tilde{v}_3)^T, \\ \tilde{B} &= \tilde{A}_2 - \tilde{A} A_1, \\ \tilde{\Sigma} &= \tilde{B}_2 - \tilde{v}_3^T \tilde{v}_3. \end{aligned}$$

The proof is given in Appendix C. Using the posterior distribution of $\mathcal{L}f$ in Lemma 4 we define the constraint probability $p_c : \mathbb{R}^{n_x} \rightarrow [0, 1]$ as

$$p_c(\mathbf{x}) = P(a(\mathbf{x}) - \nu < \xi(\mathbf{x}, X^v) < b(\mathbf{x}) + \nu) \quad (10)$$

where $\xi(\mathbf{x}, X^v) = \mathcal{L}f(\mathbf{x}^*)|Y$ for $X^v = \emptyset$ and $\xi(\mathbf{x}, X^v) = \mathcal{L}f(\mathbf{x}^*)|Y, C$ otherwise. The quantity ν is a non-negative fixed number that is included to ensure that it will be possible to increase p_c using observations with additive noise. When we use virtual observations $\tilde{C}(\mathbf{x}) =$

$\mathcal{L}f(\mathbf{x}^*) + \varepsilon^v$ that come with noise $\varepsilon^v \sim \mathcal{N}(0, \sigma_v^2)$, we can use $\nu = \max\{\sigma_v \Phi^{-1}(p_{\text{target}}), 0\}$ where $\Phi(\cdot)$ is the normal cumulative distribution function. Note that σ_v , and in this case ν , will be small numbers included mainly for numerical stability. In the numerical examples presented in this paper this noise variance was set to 10^{-6} .

In the case where $X^v = \emptyset$, computation of (10) is straightforward as $\xi(\mathbf{x}, X^v)$ is Gaussian. Otherwise we will rely on the following estimate of $p_c(\mathbf{x})$

$$\hat{p}_c(\mathbf{x}) = \frac{1}{m} \sum_{j=1}^m P(a(\mathbf{x}) - \nu < (\mathcal{L}f(\mathbf{x})|Y, C_j) < b(\mathbf{x}) + \nu) \quad (11)$$

where C_1, \dots, C_m are m samples of \mathbf{C} given in (4).

We outline an algorithm for finding a set of virtual observations X^v , such that the probability that the constraint holds locally at any $\mathbf{x} \in \Omega$ is at least p_{target} for some specified set $\Omega \subset \mathbb{R}^{n_x}$ and $p_{\text{target}} \in [0, 1)$. That is, $\min_{\mathbf{x} \in \Omega} p_c(\mathbf{x}) \geq p_{\text{target}}$. The algorithm can be used starting with no initial virtual observation locations, $X^v = \emptyset$, or using some pre-defined set $X^v \neq \emptyset$. The latter may be useful e.g. if the data Y is updated, in which case only a few additions to the previous set X^v may be needed.

Algorithm 5 *Finding locations of virtual observations X^v s.t. $\hat{p}_c(\mathbf{x}) \geq p_{\text{target}}$ for all $\mathbf{x} \in \Omega$.*

1. Compute $L = \text{Chol}(K_{X,X} + \sigma^2 I_N)$.
2. *Until convergence do:*
 - (a) If $X^v \neq \emptyset$ compute A_1 and B_1 as defined in Lemma 2, and generate m samples C_1, \dots, C_m of \mathbf{C} given in (4).
 - (b) If $X^v = \emptyset$ compute $(\mathbf{x}^*, p^*) = (\arg \min p_c(\mathbf{x}), p_c(\mathbf{x}^*))$. Otherwise compute $(\mathbf{x}^*, p^*) = (\arg \min \hat{p}_c(\mathbf{x}), \hat{p}_c(\mathbf{x}^*))$ with \hat{p}_c defined as in (11) using the samples generated in step (a).
 - (c) Terminate if $p^* \geq p_{\text{target}}$, otherwise update $X^v \rightarrow X^v \cup \{\mathbf{x}^*\}$.

The rate of convergence of Algorithm 5 relies on the probability that the constraint holds initially, $\min_{\mathbf{x}} P(a(\mathbf{x}) < (\mathcal{L}f(\mathbf{x})|Y) < b(\mathbf{x}))$, and for practical application one may monitor p^* as a function of the number of virtual observation locations, $|X^v|$, to find an appropriate stopping criterion.

3.5 Separating virtual observation locations for sub-operators

Let \mathcal{L} be the linear operator $\mathcal{L} = [\mathcal{F}_1, \dots, \mathcal{F}_k]^T$ where each \mathcal{F}_i is a linear operator leaving both the domain and range of its argument unchanged, i.e. \mathcal{F}_i produces functions from \mathbb{R}^{n_x} to \mathbb{R} , subjected to an interval constraint $[a_i(\mathbf{x}), b_i(\mathbf{x})]$. Until now we have assumed that the constrain holds at a set of virtual observation locations X^v , which means that $a_i(X^v) \leq \mathcal{F}_i f(X^v) \leq b_i(X^v)$ for all $i = 1, \dots, k$.

However, it might not be necessary to constrain each of the sub-operators \mathcal{F}_i at the same points $\mathbf{x}^v \in X^v$. Intuitively constraints with respect to \mathcal{F}_i need only be imposed at locations where $p(\mathcal{F}_i f(\mathbf{x}) \notin [a_i(\mathbf{x}), b_i(\mathbf{x})])$ is not negligible small. To accommodate this we might let X^v be the concatenation of the matrices $X^{v,1}, \dots, X^{v,k}$ and define $\mathcal{L}f(X^v) =$

$[\mathcal{F}_1 f(X^{v,1}), \dots, \mathcal{F}_k f(X^{v,1})]^T$. This is equivalent to removing of rows in $\mathcal{L}(\cdot)(X^v)$ and all of the results in this paper still apply.

In particular, the matrices needed to make use of Lemma 1 and Lemma 2 are $\mathcal{L}\mu^v$, $\mathcal{L}_2^T K_{X,X^v}$, $\mathcal{L}_2^T K_{X^*,X^v}$, and $\mathcal{L}_1 \mathcal{L}_2^T K_{X^v,X^v}$. Using that $\mathcal{F}^i f(X^v) = \mathcal{F}^i f(X^{v,i})$, these are given by

$$\begin{aligned}\mathcal{L}\mu^v &= [\mathcal{F}^1 \mu(X^{v,1}), \dots, \mathcal{F}^k \mu(X^{v,k})]^T, \\ \mathcal{L}_2^T K_{X,X^v} &= [\mathcal{F}_2^1 K_{X,X^{v,1}}, \dots, \mathcal{F}_2^k K_{X,X^{v,k}}]^T,\end{aligned}$$

where $\mathcal{L}_2^T K_{X^*,X^v}$ also is given by the above equation for $X = X^*$. Finally, $\mathcal{L}_1 \mathcal{L}_2^T K_{X^v,X^v}$ is the block matrix with blocks

$$(\mathcal{L}_1 \mathcal{L}_2^T K_{X^v,X^v})_{i,j} = \mathcal{F}_1^i \mathcal{F}_2^j K_{X^{v,i},X^{v,j}}$$

In this setting we can also improve the algorithm in Section 3.4 for finding the set of virtual observation locations by considering each sub-operator individually. To do this we will make use of the partial constraint probabilities defined as

$$\hat{p}_{c,i}(\mathbf{x}) = \frac{1}{m} \sum_{j=1}^m P(a_i(\mathbf{x}) - \nu < (\mathcal{L}f(\mathbf{x})|Y, C_j)_i < b_i(\mathbf{x}) + \nu) \quad (12)$$

where $(\mathcal{L}f(\mathbf{x})|Y, C_j)_i$ is the univariate Normal distribution given by the i -th row of $(\mathcal{L}f(\mathbf{x})|Y, C_j)$ and C_1, \dots, C_m are m samples of \mathbf{C} given in (4) as before. Similarly, $p_{c,i}(\mathbf{x})$ can be defined as in (10) by considering only the i -th sub-operator. In the case where $X^v = \emptyset$ this means that $\xi(\mathbf{x}, X^v) = \mathcal{F}_i f(\mathbf{x}^*)|Y$.

For the individual sub-operators \mathcal{F}_i , the set of virtual observations X_i^v needed to ensure that $\hat{p}_{c,i}(\mathbf{x}) \geq p_{\text{target}}$ can then be found using the following algorithm.

Algorithm 6 Finding locations of virtual observations X_i^v s.t. $\hat{p}_{c,i}(\mathbf{x}) \geq p_{\text{target}}$ for all $\mathbf{x} \in \Omega$ and all sub-operators $\mathcal{F}_1, \dots, \mathcal{F}_k$.

1. Compute $L = \text{Chol}(K_{X,X} + \sigma^2 I_N)$.
2. Until convergence do:
 - (a) If $X^v \neq \emptyset$ compute A_1 and B_1 as defined in Lemma 2, and generate m samples C_1, \dots, C_m of \mathbf{C} given in (4).
 - (b) If $X^v = \emptyset$ compute $(\mathbf{x}_i^*, p_i^*) = (\arg \min p_{c,i}(\mathbf{x}), p_{c,i}(\mathbf{x}^*))$. Otherwise compute $(\mathbf{x}_i^*, p_i^*) = (\arg \min \hat{p}_{c,i}(\mathbf{x}), \hat{p}_{c,i}(\mathbf{x}^*))$, for all $i = 1, \dots, k$ with $\hat{p}_{c,i}$ defined as in (12) using the samples generated in step (a).
 - (c) Let (\mathbf{x}^*, p^*, j) correspond to the smallest probability: $p^* = p_j^* = \min_i p_i^*$.
 - (d) Terminate if $p^* \geq p_{\text{target}}$, otherwise update $X_j^v \rightarrow X_j^v \cup \{\mathbf{x}^*\}$.

Using Algorithm 6 instead of Algorithm 5 will provide a more optimal set of virtual observation locations. However, if one were to impose conflicting constraints there is no guarantee of convergence in the sense that adding virtual locations for one constraint may

reduce the probability $\hat{p}_{c,i}(\mathbf{x})$ for another. For practical applications it might be wise to monitor p_i^* as a function of the points added, as this will reveal conflicting constraints or constraints that does not agree with the training data. Moreover, if convergence is slow (i.e. many virtual locations are needed) this might suggest that the prior GP is not suitable.

3.6 Prediction using the posterior distribution

For the unconstrained GP in this paper where the likelihood is given by Gaussian white noise, the posterior mean and covariance is sufficient to describe predictions as the posterior remains Gaussian. It is also known that in this case there is a correspondence between the posterior mean of the GP and the optimal estimator in the Reproducing Kernel Hilbert Space (RKHS) associated with the GP (Kimeldorf and Wahba, 1970). Interestingly, a similar correspondence holds for the constrained case. Maatouk et al. (2016) show that for constrained interpolation, the Maximum *A Posteriori* (MAP) or mode of the posterior is the optimal constrained interpolation function in the RKHS. This holds when the GP is constrained to a convex set of functions, which is the case in this paper where we condition on linear transformations of a function restricted to a convex set.

4. Gaussian process modelling with boundedness and monotonicity constraints

In this section we present some examples related to function estimation where we assume that the function and some of its partial derivatives are bounded. This is also the scenario considered in the literature on shape constrained GPs: One approach by Golchi et al. (2015), based on a similar idea as Riihimki and Vehtari (2010), make use of a *probit* link to represent interval observations of function derivatives. Here Golchi et al. (2015) estimate the exact posterior from sampling, whereas Riihimki and Vehtari (2010) make use of expectation propagation for approximate inference. A different approach is taken by Da Veiga and Marrel (2012, 2015), where only truncated moments of the constrained process are approximated. Maatouk and Bay (2017) and López-Lopera et al. (2018) on the other hand set out to model a conditional process where the constraints hold in the entire domain, as opposed to at a finite set of virtual locations. They achieve this by make use of finite-dimensional approximations of the GP that converge uniformly pathwise. Some other alternatives can also be found in (Lenk and Choi, 2017; Abrahamsen and Benth, 2001; Lin and Dunson, 2014). In the setting where we condition on the derivative process our approach is most similar to that in (Wang and Berger, 2016), where the authors make use of a similar sampling scheme for noiseless GP regression applied to computer code emulation.

In this section we will make us of the following constraints:

- $a_0(\mathbf{x}) \leq f(\mathbf{x}) \leq b_0(\mathbf{x})$
- $a_i(\mathbf{x}) \leq \partial f / \partial x_i(\mathbf{x}) \leq b_i(\mathbf{x})$

for all \mathbf{x} in some bounded subset of \mathbb{R}^{n_x} , and $i \in \mathcal{I} \subset \{1, \dots, n_x\}$. Without loss of generality we assume that the constrains on partial derivatives are with respect to the first k components of \mathbf{x} , i.e. $\mathcal{I} = \{1, \dots, k\}$ for some $k \leq n_x$.

As the prior GP we will assume a constant mean $\mu = 0$ and the squared exponential covariance function, also called radial basis function (RBF) kernel, given by

$$K(\mathbf{x}, \mathbf{x}') = \sigma_K^2 e^{-\frac{1}{2} \sum (\frac{x_i - x'_i}{l_i})^2}, \quad (13)$$

with variance parameter σ_K^2 and length scale parameters l_i for $i = 1, \dots, n_x$. With this choice of covariance function existence of the transformed GP is ensured. In fact, the resulting process is infinitely differentiable (see Adler, 1981, Theorem 2.2.2). This prior GP was chosen as it is the one most commonly used in the literature, and thus a good starting point for illustrating the effect of including linear constraints. We note that although it is not in general possible to design mean and covariance functions that produce GPs that satisfy the constraints considered in this paper, one could certainly ease numerical computations by selecting a GP prior based on the constraint probability $p(C|Y, \theta)$ in (5), and for instance make us of a mean function that is known to satisfy the constraint.

If we let $\mathcal{F}^0 f = f$, $\mathcal{F}^i f = \partial f / \partial x_i$ and $X^{v,i}$ be the set of m_i virtual observations corresponding to the i -th operator \mathcal{F}^i , then we can make use of the equations in Section 3.5 to obtain

$$\mathcal{L}\mu^v = [\mu \mathbf{1}_{m_0}, \mathbf{0}_{m_{[1,k]}}]^T$$

where $\mathbf{1}_{m_1}$ is the vector $[1, \dots, 1]^T$ of length m_1 and $\mathbf{0}_{m_{[1,k]}}$ is the vector $[0, \dots, 0]^T$ of length $m_{[1,k]} = -m_0 + \sum m_i$. Furthermore,

$$\mathcal{L}_2^T K_{X, X^v} = \left[K_{X, X^{v,0}}, (K_{X^{v,1}, X}^{1,0})^T, \dots, (K_{X^{v,k}, X}^{k,0})^T \right],$$

$$\mathcal{L}_2^T K_{X^*, X^v} = \left[K_{X^*, X^{v,0}}, (K_{X^{v,1}, X^*}^{1,0})^T, \dots, (K_{X^{v,k}, X^*}^{k,0})^T \right],$$

and

$$\mathcal{L}_1 \mathcal{L}_2^T K_{X^v, X^v} = \begin{bmatrix} K_{X^{v,0}, X^{v,0}} & (K_{X^{v,1}, X^{v,0}}^{1,0})^T & \cdots & (K_{X^{v,k}, X^{v,0}}^{k,0})^T \\ K_{X^{v,1}, X^{v,0}}^{1,0} & K_{X^{v,1}, X^{v,1}}^{1,1} & \cdots & K_{X^{v,1}, X^{v,k}}^{1,k} \\ \vdots & \vdots & \ddots & \vdots \\ K_{X^{v,k}, X^{v,0}}^{k,0} & K_{X^{v,k}, X^{v,0}}^{k,1} & \cdots & K_{X^{v,k}, X^{v,k}}^{k,k} \end{bmatrix},$$

where we have used the notation

$$K^{i,0}(\mathbf{x}, \mathbf{x}') = \frac{\partial}{\partial x_i} K(\mathbf{x}, \mathbf{x}') \text{ and } K^{i,j}(\mathbf{x}, \mathbf{x}') = \frac{\partial^2}{\partial x_i \partial x'_j} K(\mathbf{x}, \mathbf{x}').$$

The use of constraints related to boundedness and monotonicity is illustrated using two examples of GP regression. Example 1 considers a function $f: \mathbb{R} \rightarrow \mathbb{R}$ subjected to boundedness and monotonicity constraints. In Example 2 a function $f: \mathbb{R}^4 \rightarrow \mathbb{R}$ is estimated under the assumption information on whether the function is monotone increasing or decreasing as a function of the first two inputs is known, i.e. $\text{sgn}(\partial f / \partial x_1)$ and $\text{sgn}(\partial f / \partial x_2)$ is known.

Example 1

As a simple illustration of imposing constraints in GP regression we first consider a function

$f: \mathbb{R} \rightarrow \mathbb{R}$ given by $f(x) = \frac{1}{3}[\tan^{-1}(20x - 10) - \tan^{-1}(-10)]$. We assume that the function value is known at 7 input locations given by $x_i = 0.1 + 1/(i + 1)$ for $i = 1, \dots, 7$. First we assume that the observations are noiseless, i.e. $f(x_i)$ is observed for each x_i . Estimating the function that interpolates at these observations is commonly referred to as *emulation*, which is relevant when dealing with data from computer experiments. Our function $f(x)$ is both bounded and increasing on all of \mathbb{R} . In this example we will constrain the GP to satisfy the conditions that for $x \in [0, 1]$ we have that $df/dx \geq 0$ and $a(x) \leq f(x) \leq b(x)$ for $a(x) = 0$ and $b(x) = \frac{1}{3}\ln(30x + 1) + 0.1$. The function is shown in Figure 1 together with the bounds and the 7 observations.

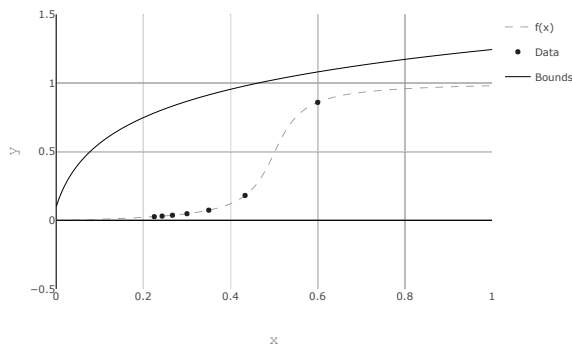


Figure 1: Function to emulate in Example 1

We select an RBF kernel (13) with parameters $\sigma_K = 0.5$ (variance) and $l = 0.1$ (length scale). To represent noiseless observations we set $\sigma^2 = 10^{-6}$, where σ^2 is the noise variance in the Gaussian likelihood. The assumed noise on virtual observations will also be set to 10^{-6} . Figure 2 shows the resulting GP in sub-figures a_1 and a_2 . To illustrate the effect of adding constraints we show the constrained GP using only boundedness constraint, only monotonicity constraint and finally when both constraints are imposed simultaneously. Algorithm 6 was used with a target probability $p_{target} = 0.99$ to determine the virtual observation locations that are indicated in the figures, and the posterior mode was computed by maximizing a Gaussian kernel density estimator over the samples generated in Algorithm 3. For both constraints (sub-figure d_1 and d_2) 17 locations was needed for monotonicity and only 3 locations was needed to impose boundedness when the virtual locations for both constraints were optimized simultaneously. This is reasonable as requiring $f(0) > 0$ is sufficient to ensure $f(x) > 0$ for $x \geq 0$ when f is increasing, and similarly requiring $f(x^v) < b(x^v)$ for some few points $x^v \in [0.6, 1]$ should suffice.

For illustration purposes none of the hyperparameters of the GP were optimized. Moreover, for datasets such as the one in this example using plug-in estimates obtained from MLE generally not appropriate due to overfitting. Maximizing the marginal likelihood for the unconstrained GP (Eq. (7)) gave a very poor model upon visual inspection ($\sigma_K = 0.86, l = 0.26$). However, it was observed that the estimated parameters for the constrained model (using Eq. (6)) gives estimates closer to the selected prior which seems more reason-

able ($\sigma_K = 0.42, l = 0.17$), and hence the inclusion of the constraint probability, $p(C|Y, \theta)$, in the likelihood seems to improve the estimates also for the unconstrained GP.

We may also assume that the observations come with Gaussian white noise, which in terms of numerical stability is much less challenging than interpolation. Figure 3 shows the resulting GPs fitted to 50 observations. The observations were generated by sampling $x_i \in [0.4, 0.7]$ uniformly, and y_i from $f(x_i) + \varepsilon_i$ where ε_i are i.i.d. zero mean Gaussian with variance $\sigma^2 = 0.04$. Both GPs were optimized using plug-in estimates of hyperparameters (σ_K, l, σ^2) given by maximizing the marginal likelihood. These are ($\sigma_K = 0.34, l = 0.32, \sigma^2 = 0.053$) for the constrained case and ($\sigma_K = 0.34, l = 0.23, \sigma^2 = 0.040$) for the unconstrained case. We observe that the estimated noise variance is larger in the constrained model than the unconstrained where this estimate is exact.

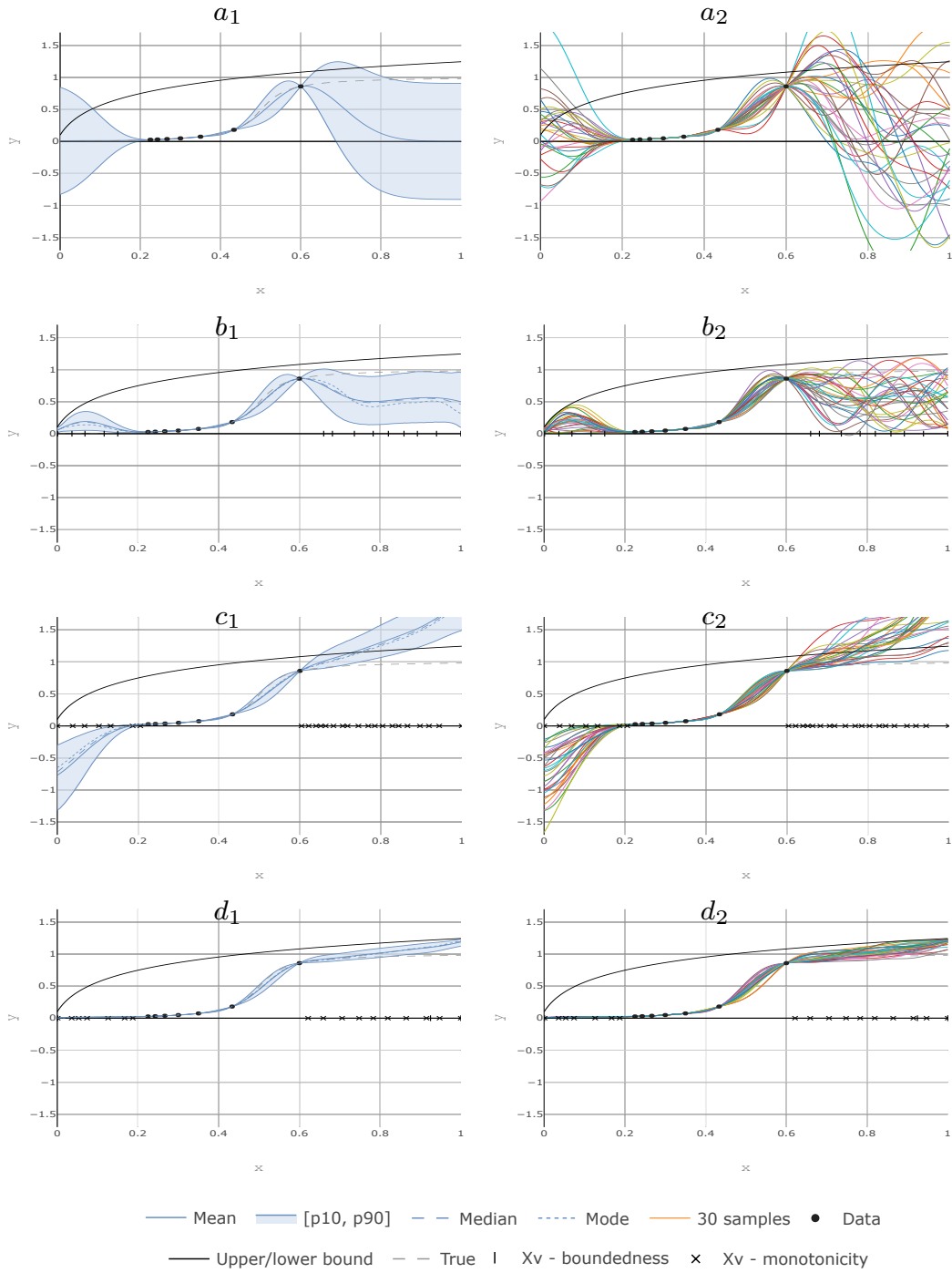


Figure 2: The GP with parameters $\sigma_K = 0.5$ (variance) and $l = 0.1$ (length scale) used in Example 1. Figures a_i show the unconstrained GP, whereas b_i , c_i and d_i show the constrained GPs for boundedness, monotonicity and both boundedness and monotonicity respectively. The virtual observation locations are indicated by markers on the x-axis.

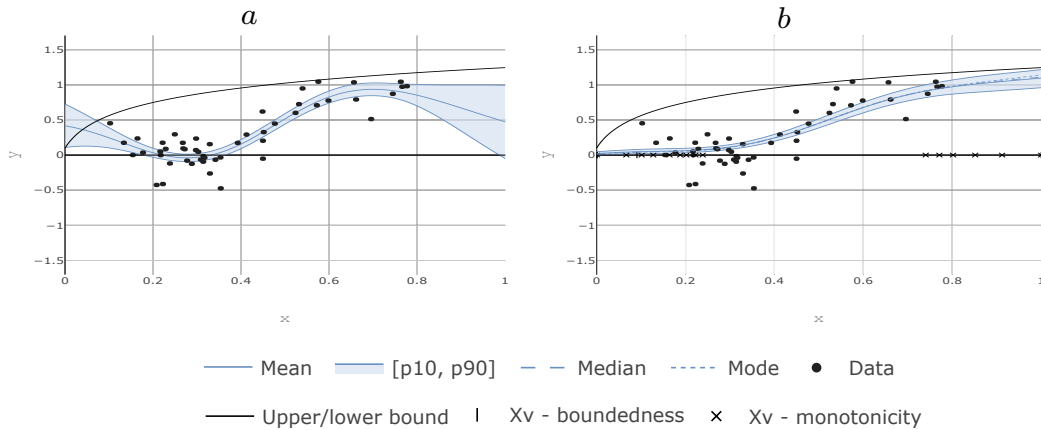


Figure 3: Unconstrained (a) and constrained (b) GPs fitted to 50 observations with Gaussian noise. The predictive distributions are shown, i.e. the distribution of $f(x)$ where $y = f(x) + \varepsilon$.

Example 2

In this example we consider emulation of a function $f : \mathbb{R}^4 \rightarrow \mathbb{R}$, where we assume that the sign of the first two partial derivatives, $\text{sgn}(\partial f/\partial x_1)$ and $\text{sgn}(\partial f/\partial x_2)$, are known. The function to emulate is

$$f(\mathbf{x}) = \sum_{i=1}^m L_i \cos \left(\sum_{j=1}^i \tau_j \right),$$

for $m = 2$, and $\mathbf{x} = [L_1, L_2, \tau_1, \tau_2]$. The function is inspired by the robot arm function often used to test function estimation (An and Owen, 2001). Here $f(\mathbf{x})$ is the y-coordinate of a two dimensional robot arm with m line segments of length $L_i \in [0, 1]$ positioned at angle $\tau_i \in [0, 2\pi]$ with respect to the horizontal axis. The constraints on the first two partial derivatives thus implies that it is known whether or not the arm will move further away from the x-axis, as a function of the arm lengths, L_1 and L_2 , for any combination of τ_1 and τ_2 .

First, an unconstrained GP was fitted using 40 observations taken from a latin hypercube sample over the input space $[0, 1]^2 \times [0, 2\pi]^2$, and plug-in hyperparameters ($\sigma_K = 0.41, l_1 = 0.98, l_2 = 1.10, l_3 = 0.16, l_4 = 0.23$) were found by MLE. The constrained GP was determined by first generating a new latin hypercube sample of 40 observations to use as a seed set for virtual observation locations for constraining both derivatives $\partial f/\partial x_1$ and $\partial f/\partial x_2$. Hyperparameters were then optimized before searching for additional virtual observation locations ($\sigma_K = 0.80, l_1 = 1.59, l_2 = 1.14, l_3 = 0.21, l_4 = 0.28$). The performance of each model can be assessed visually by comparing predictions for randomly selected inputs. The result for 100 randomly selected predictions are shown in Figure 4. As expected the estimated prediction uncertainty is reduced significantly using the constrained model, and single predictions given by the posterior mean are also improved.

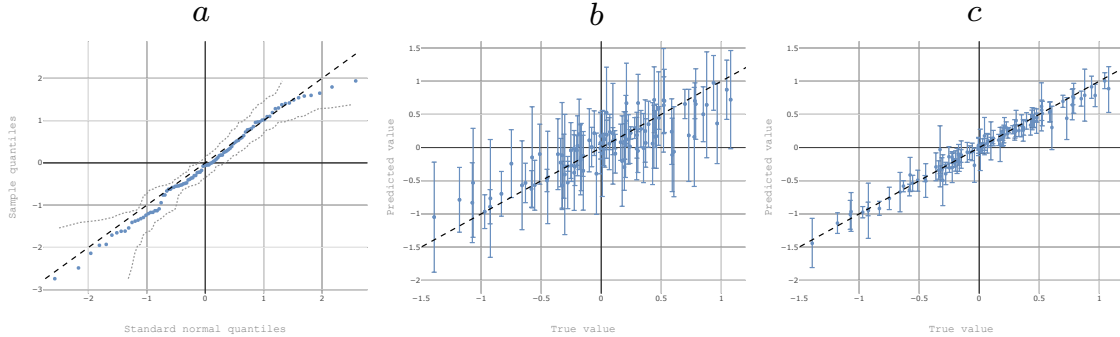


Figure 4: Figure *a* shows a qq-plot with 95% confidence band of 100 normalized residuals $(y_i - \mu_i)/(\sigma_i)$, where μ_i and σ_i^2 are the mean and variance of the predictive distribution of the unconstrained GP. In Figure *b* predictions vs the true function value is shown together with a $[0.025, 0.975]$ (95%) percentile interval for the unconstrained GP. The same type of figure is shown in *c* for the constrained GP.

5. Discussion

The model presented in this paper provides a consistent approach to GP regression under multiple linear constraints. The computational framework used is based on sampling, which has the convenient property of being exact in the limit. However, sampling strategies like the one in this paper can be too numerically demanding as opposed to approximation methods such as Laplace approximations, variational Bayesian inference, expectation propagation etcetera. The choice of using a sampling-based approach came from the author’s intended use, which relates to machine learning for high-risk and safety-critical engineering applications. In this scenario it is essential that the accuracy of numerical estimation- or approximation methods can be assessed. And in the case where simulation-based methods cannot be used due to computational limitations, they still serve as a useful benchmark that can help in the development of suitable approximation-based algorithms. As for the simulation scheme in this paper, the only computational burden lies in sampling from a truncated multivariate Gaussian. As this is a fairly general problem multiple good samplers exist for this purpose.

Since our model is based on the use of virtual observation locations, we are aware that the task of estimating or optimizing model hyperparameters in general is not well defined. This is because the likelihood depends both on the hyperparameters and the set of virtual observation locations (Eq. (6)). Although we only consider hyperparameter optimization by MLE in this paper, this problem arises also in the fully Bayesian setting, in the sense that the posterior over hyperparameters will depend on the set of virtual observation locations. This problem is neglected in the literature on shape constrained GPs, where it is either assumed that the virtual observation locations are known a priori (for low input dimension selecting a space filling sufficiently dense design is unproblematic), or the hyperparameters are addressed independently of these (which in our case would be using the unconstrained

MLE). To our knowledge the problem of simultaneously estimating hyperparameters and virtual observation locations has not yet been addressed. A rather simplistic approach is to iterate between estimating hyperparameter and the set of virtual observation locations. However, for higher input dimensions this might be problematic altogether, in which case sparse approximations may be needed to deal with a large set of virtual observation locations. In this setting it might be more fruitful to view the virtual observations as additional hyperparameters, in a model approximating the posterior corresponding to an infinite and properly dense set of virtual observation locations, e.g. as in the inducing points framework for scaling GPs to large datasets (G. de G. Matthews et al., 2015). This is a topic of further research.

Finally, we note that the model presented in this paper relies on conditioning on a transformed GP with values in \mathbb{R}^{n_c} , and could be extended to multi-output GPs over functions $f: \mathbb{R}^{n_x} \rightarrow \mathbb{R}^{n_y}$ in a natural way. We also derive the exact formula for the constraint probability, $p(C|Y)$, which is interesting in its own for investigating whether constraints such as e.g. monotonicity are likely to hold given a set of observations. Alternatively, inference on the constraint noise parameter σ_v can provide similar type of information.

Acknowledgments

This work has been supported by grant 276282 from the Norwegian Research Council and DNV GL Group Technology and Research. The research is part of an initiative on applying constraints based on phenomenological knowledge in probabilistic machine learning for high-risk applications, and the author would like to thank colleagues at DNV GL and the University of Oslo for fruitful discussions on the topic. A special thanks to Arne B. Huseby, Simen Eldevik and Andreas Hafver for commenting on the paper.

Appendices

A. Proof of Lemma 1

We start by observing that $(\mathbf{f}^*, \tilde{C}, Y)$ is jointly Gaussian with mean and covariance

$$\mathbb{E}([\mathbf{f}^*, \tilde{C}, Y]^T) = [\mu^*, \mathcal{L}\mu^v, \mu]^T, \quad (14)$$

$$\text{cov}([\mathbf{f}^*, \tilde{C}, Y]^T) = \begin{bmatrix} K_{X^*, X^*} & \mathcal{L}_2^T K_{X^*, X^v} & K_{X^*, X} \\ \mathcal{L}_1 K_{X^v, X^*} & \mathcal{L}_1 \mathcal{L}_2^T K_{X^v, X^v} + \sigma_v^2 I_{N_v n_c} & \mathcal{L}_1 K_{X^v, X} \\ K_{X, X^*} & \mathcal{L}_2^T K_{X, X^v} & K_{X, X} + \sigma^2 I_N \end{bmatrix}. \quad (15)$$

By first conditioning on Y we obtain

$$[\mathbf{f}^*, \tilde{C}|Y]^T \sim \mathcal{N} \left(\begin{bmatrix} \mu^* + A_2(Y - \mu) \\ \mathcal{L}\mu^v + A_1(Y - \mu) \end{bmatrix}, \begin{bmatrix} B_2 & B_3 \\ B_3^T & B_1 \end{bmatrix} \right), \quad (16)$$

for $A_1 = (\mathcal{L}_1 K_{X^v, X})(K_{X, X} + \sigma^2 I_N)^{-1}$, $A_2 = K_{X^*, X}(K_{X, X} + \sigma^2 I_N)^{-1}$, $B_1 = \mathcal{L}_1 \mathcal{L}_2^T K_{X^v, X^v} + \sigma_v^2 I_{N_v n_c} - A_1 \mathcal{L}_2^T K_{X, X^v}$, $B_2 = K_{X^*, X^*} - A_2 K_{X, X^*}$, and $B_3 = \mathcal{L}_2^T K_{X^*, X^v} - A_2 \mathcal{L}_2^T K_{X, X^v}$.

Conditioning on \tilde{C} then gives

$$\mathbf{f}^*|Y, \tilde{C} \sim \mathcal{N}\left(\mu^* + A(\tilde{C} - \mathcal{L}\mu^v) + B(Y - \mu), \Sigma\right), \quad (17)$$

for $A = B_3 B_1^{-1}$, $B = A_2 - A A_1$ and $\Sigma = B_2 - A B_3^T$.

Similarly, we may derive $\tilde{C}|Y$ by observing that the joint distribution of \tilde{C}, Y is given by removing the first row in (14) and the first row and column in (15). Hence,

$$\tilde{C}|Y \sim \mathcal{N}(\mathcal{L}\mu^v + A_1(Y - \mu), B_1). \quad (18)$$

The constrained posterior of \tilde{C} is obtained by applying the constraint C to the posterior, and hence $\tilde{C}|Y, C$ becomes a truncated Gaussian with the same mean and variance as in (18), and the bounds $a(X^v)$ and $b(X^v)$ given by C . Similarly, $\mathbf{f}^*|Y, C$ is obtained by replacing \tilde{C} in (17) with $\tilde{C}|Y, C$. Finally, the probability $p(C|Y)$ is just the probability that $\tilde{C}|Y$ given in (18) falls within the bounds given by C , and the unconstrained distribution remains the same as (2). \blacksquare

B. Proof of Lemma 2

The equations in Lemma 2 can be verified by simply inserting L , v_1 and v_2 and check against the expressions in Lemma 1. We show this for A_1 and B_1 , and the results for the remaining matrices are proved by applying the same procedures. In order to factorize B_1 we use that B_1 is the covariance matrix of a Gaussian random variable (see (18) in Appendix A), and must therefore be symmetric and positive definite.

To show that $A_1 = (L^T \setminus v_1)^T$ we use that $v_1 = L \setminus \mathcal{L}_2^T K_{X, X^v} \Rightarrow L v_1 = \mathcal{L}_2^T K_{X, X^v}$. Hence,

$$\begin{aligned} A_1 &= (L^T \setminus v_1)^T \\ &\Rightarrow L^T A_1^T = v_1 = L \setminus \mathcal{L}_2^T K_{X, X^v} \\ &\Rightarrow L L^T A_1^T = \mathcal{L}_2^T K_{X, X^v} \\ &\Rightarrow A_1 = ((L L^T)^{-1} \mathcal{L}_2^T K_{X, X^v})^T = (\mathcal{L}_1 K_{X^v, X})(K_{X, X} + \sigma^2 I_N)^{-1} \end{aligned}$$

where we have used that $(\mathcal{L}_2^T K_{X, X^v})^T = \mathcal{L}_1 K_{X^v, X}$ and $L L^T = K_{X, X} + \sigma^2 I_N$.

To show that $B_1 = \mathcal{L}_1 \mathcal{L}_2^T K_{X^v, X^v} + \sigma_v^2 I_{N_v n_c} - v_1^T v_1$ we need to show that $v_1^T v_1 = A_1 \mathcal{L}_2^T K_{X, X^v}$, which is trivial

$$\begin{aligned} v_1^T v_1 &= (L^{-1} \mathcal{L}_2^T K_{X, X^v})^T (L^{-1} \mathcal{L}_2^T K_{X, X^v}) \\ &= \mathcal{L}_1 K_{X^v, X} (L L^T)^{-1} \mathcal{L}_2^T K_{X, X^v} \\ &= A_1 \mathcal{L}_2^T K_{X, X^v} \end{aligned}$$

■

C. Proof of Lemma 4

This follows exactly from the proofs of Lemma 1 and Lemma 2 by replacing $\mathbf{f}^* \rightarrow \mathcal{L}f(\mathbf{x}^*)$, which implies $\mu^* \rightarrow \mathcal{L}\mu^*$, $K_{X^*,X} \rightarrow \mathcal{L}_1 K_{\mathbf{x}^*,X}$, $K_{X^*,X^*} \rightarrow \mathcal{L}_1 \mathcal{L}_2^T K_{\mathbf{x}^*,\mathbf{x}^*}$ and $\mathcal{L}_2^T K_{X^*,X^v} \rightarrow \mathcal{L}_1 \mathcal{L}_2^T K_{\mathbf{x}^*,X^v}$.

■

References

- Petter Abrahamsen and Fred Espen Benth. Kriging with inequality constraints. *Mathematical Geology*, 33(6):719–744, Aug 2001. ISSN 1573-8868. doi: 10.1023/A:1011078716252. URL <https://doi.org/10.1023/A:1011078716252>.
- R.J. Adler. *The geometry of random fields*. Wiley series in probability and mathematical statistics. Probability and mathematical statistics. J. Wiley, 1981. ISBN 9780471278443. URL <https://books.google.no/books?id=SxXvAAAAAAAJ>.
- Christian Agrell, Simen Eldevik, Andreas Hafver, Frank Børre Pedersen, and Erik Stensrud. Pitfalls of machine learning for tail events in high risk environments. In Stein Haugen, Anne Barros, Coen van Gulijk, Trond Kongsvik, and Jan Erik Vinnem, editors, *Safety and Reliability Safe Societies in a Changing World - Proceedings of ESREL 2018*. CRC Press, june 2018. ISBN 978-0815386827.
- Jian An and Art Owen. Quasi-regression. *Journal of Complexity*, 17(4):588 – 607, 2001. ISSN 0885-064X. doi: <https://doi.org/10.1006/jcom.2001.0588>. URL <http://www.sciencedirect.com/science/article/pii/S0885064X01905886>.
- François Bachoc, Agnes Lagnoux, and Andrés F. López-Lopera. Maximum likelihood estimation for gaussian processes under inequality constraints. working paper or preprint, August 2018. URL <https://hal.archives-ouvertes.fr/hal-01864340>.
- Z. I. Botev. The normal law under linear restrictions: simulation and estimation via mini-max tilting. *Journal of the Royal Statistical Society: Series B (Statistical Methodology)*, 79(1):125–148, 2017. doi: 10.1111/rssb.12162. URL <https://rss.onlinelibrary.wiley.com/doi/abs/10.1111/rssb.12162>.
- Sébastien Da Veiga and Amandine Marrel. Gaussian process modeling with inequality constraints. *Annales de la faculté des sciences de Toulouse Mathématiques*, 21(3):529–555, 4 2012. URL <http://eudml.org/doc/250989>.
- Sébastien Da Veiga and Amandine Marrel. Gaussian process regression with linear inequality constraints. working paper or preprint, 10 2015. URL <https://hal.archives-ouvertes.fr/hal-01515468>.
- Simen Eldevik, Christian Agrell, Andreas Hafver, and Frank B. Pedersen. AI + Safety: Safety implications for artificial intelligence and why we need to combine casual- and data-

- driven models. 08 2018. URL <https://ai-and-safety.dnvgl.com/>. [Online position paper by DNV GL Group Technology and Research; posted 28-August-2018].
- Alexander G. de G. Matthews, James Hensman, Richard Turner, and Zoubin Ghahramani. On sparse variational methods and the kullback-leibler divergence between stochastic processes. 04 2015. doi: 10.17863/CAM.15597.
- Zoubin Ghahramani. Probabilistic machine learning and artificial intelligence. *Nature*, 521(7553):452–459, 2015. doi: 10.1038/nature14541. URL <https://doi.org/10.1038/nature14541>.
- Shirin Golchi, D R. Bingham, H Chipman, and David Campbell. Monotone emulation of computer experiments. *SIAM/ASA Journal on Uncertainty Quantification*, 3:370–392, 01 2015.
- Carl Jidling, Niklas Wahlström, Adrian Wills, and Thomas B Schön. Linearly constrained gaussian processes. pages 1215–1224. Curran Associates, Inc., 2017. URL <http://papers.nips.cc/paper/6721-linearly-constrained-gaussian-processes.pdf>.
- Marc C. Kennedy and Anthony O’Hagan. Bayesian calibration of computer models. *Journal of the Royal Statistical Society: Series B (Statistical Methodology)*, 63(3):425–464, 2001. doi: 10.1111/1467-9868.00294. URL <https://rss.onlinelibrary.wiley.com/doi/abs/10.1111/1467-9868.00294>.
- George S. Kimeldorf and Grace Wahba. A correspondence between bayesian estimation on stochastic processes and smoothing by splines. *Ann. Math. Statist.*, 41(2):495–502, 04 1970. doi: 10.1214/aoms/1177697089. URL <https://doi.org/10.1214/aoms/1177697089>.
- J. H. Kotecha and P. M. Djuric. Gibbs sampling approach for generation of truncated multivariate gaussian random variables. In *1999 IEEE International Conference on Acoustics, Speech, and Signal Processing. Proceedings. ICASSP99 (Cat. No.99CH36258)*, volume 3, pages 1757–1760 vol.3, March 1999. doi: 10.1109/ICASSP.1999.756335.
- Gyemin Lee and Clayton Scott. Em algorithms for multivariate gaussian mixture models with truncated and censored data. *Computational Statistics & Data Analysis*, 56(9):2816 – 2829, 2012. ISSN 0167-9473. doi: <https://doi.org/10.1016/j.csda.2012.03.003>. URL <http://www.sciencedirect.com/science/article/pii/S0167947312001156>.
- Peter Lenk and Taeryon Choi. Bayesian analysis of shape-restricted functions using gaussian process priors. *Statistica Sinica*, 27:43–69, 2017.
- Lizhen Lin and David B. Dunson. Bayesian monotone regression using gaussian process projection. *Biometrika*, 101(2):303–317, 2014. doi: 10.1093/biomet/ast063. URL <http://dx.doi.org/10.1093/biomet/ast063>.
- A. López-Lopera, F. Bachoc, N. Durrande, and O. Roustant. Finite-dimensional gaussian approximation with linear inequality constraints. *SIAM/ASA Journal on Uncertainty Quantification*, 6(3):1224–1255, 2018. doi: 10.1137/17M1153157. URL <https://doi.org/10.1137/17M1153157>.

- Hassan Maatouk and Xavier Bay. Gaussian process emulators for computer experiments with inequality constraints. *Mathematical Geosciences*, 49(5):557–582, Jul 2017. ISSN 1874-8953. doi: 10.1007/s11004-017-9673-2. URL <https://doi.org/10.1007/s11004-017-9673-2>.
- Hassan Maatouk, Laurence Grammont, and Xavier Bay. Generalization of the kimeldorf-wahba correspondence for constrained interpolation. *Electronic Journal of Statistics*, 10(1):1580–1595, 2016.
- G. Matheron. The intrinsic random functions and their applications. *Advances in Applied Probability*, 5(3):439–468, 1973. ISSN 00018678. URL <http://www.jstor.org/stable/1425829>.
- A. Papoulis and S. U. Pillai. *Probability, Random Variables, and Stochastic Processes*. McGraw-Hill Higher Education, 4 edition, 2002.
- Carl Edward Rasmussen and Christopher K. I. Williams. *Gaussian Processes for Machine Learning (Adaptive Computation and Machine Learning)*. The MIT Press, 2005. ISBN 026218253X.
- Jaakko Riihimäki and Aki Vehtari. Gaussian processes with monotonicity information. *Journal of Machine Learning Research - Proceedings Track*, 9:645–652, 01 2010.
- Jerome Sacks, William J. Welch, Toby J. Mitchell, and Henry P. Wynn. Design and analysis of computer experiments. *Statist. Sci.*, 4(4):409–423, 11 1989. doi: 10.1214/ss/1177012413. URL <https://doi.org/10.1214/ss/1177012413>.
- Simo Särkkä. Linear operators and stochastic partial differential equations in gaussian process regression. In Timo Honkela, Włodzisław Duch, Mark Girolami, and Samuel Kaski, editors, *Artificial Neural Networks and Machine Learning – ICANN 2011*, pages 151–158, Berlin, Heidelberg, 2011. Springer Berlin Heidelberg. ISBN 978-3-642-21738-8.
- Philip Duncan Thompson. Optimum smoothing of two-dimensional fields. *Tellus*, 8(3):384–393, 1956. doi: 10.1111/j.2153-3490.1956.tb01236.x. URL <https://onlinelibrary.wiley.com/doi/abs/10.1111/j.2153-3490.1956.tb01236.x>.
- Xiaojing Wang and James O. Berger. Estimating shape constrained functions using gaussian processes. *SIAM/ASA Journal on Uncertainty Quantification*, 4:1–25, 01 2016.